Available online at www.elixirpublishers.com (Elixir International Journal)

Applied Mathematics

Elixir Appl. Math. 36 (2011) 3468-3475

ISSN: 2229-712X

Perturbation analysis of MHD mixed convective slip flow in a permeable vertical plate with Joule heating and soret effect

B.Rushi Kumar and R. Sivaraj

Fluid Dynamics Division, School of Advanced Sciences, VIT University, Vellore – 632 014, India.

ARTICLE INFO

Article history:

Received: 16 May 2011;

Received in revised form:

7 July 2011;

Accepted: 16 July 2011;

Keywords

MHD,

Slip flow,

Mixed convection,

Joule heating,

Soret effect.

ABSTRACT

This paper is focused on the study of mixed convective heat and mass transfer on the steady MHD flow of a heat absorbing fluid in a permeable vertical plate subject to the influence of buoyancy, viscous dissipation, Joule heating and Soret effect embedded with slip condition at the boundary layer. The momentum, energy and mass diffusion equations are coupled non-linear partial differential equations which are solved by perturbation technique. The effect of skin friction, Nusselt number and Sherwood number distributions are shown in tables. The numerical results are shown on graphs. The effects of various significant parameters entering into the problem have been discussed in detail.

Introduction

MHD heat transfer has gained significance owing to applications in recent advancement of space technology. In recent years, progress has been considerably made in the study of heat and mass transfer with magneto hydrodynamic flows due to its application in many devices, like the MHD power generator and Hall accelerator. We can realize the influence of magnetic field from the work of (Barletta et al. [1], Afify [2], Srinivas Muthuraj [3], Prakash [4]). Mixed convection arises in many natural and technological processes, depending on the forced flow direction, the buoyancy forces may aid or oppose the forced flow, causing an increase or decrease in the heat transfer rates. The problem of mixed convection resulting from flow over a heated vertical plate is of considerable theoretical and practical interest. Mixed convection problems involve with different configurations have investigated by (Yih [5], Barletle [6], Chin [7], Motsa [8]). The Soret effect has gained considerable interest in convective heat and mass transfer of Newtonian fluids and it is significant when density differences exist in the flow regime. Soret effect is important in coupled heat and mass transfer of low and intermediate molecular weight gases and it has more significant in binary systems, geophysical systems, encountered in chemical process engineering and also in high-speed aerodynamics. (Kafoussias and Williams [9], Angel [10], Alam and Rahman [11], Mansour et al. [12]) have shown the significant of Soret effect in various studies.

Transport phenomena involving the combined influence of thermal and solutal buoyancy are often encountered in many engineering systems and natural environments. There are many applications of such transport processes in the industry, notably in heat exchangers, solar energy collectors and thermal protection systems. The interaction of buoyancy has increased greatly during the last decade due to its importance in many practical applications. The effect of buoyancy has been analyzed for different problems by (Alimi [13], Shateyi [14], Elzubier et al. [15], Muthuraj and Srinivas [16]). Joule heating is a developing technology with considerable potential for the food industry. The main advantages of ohmic processing are the rapid and relatively uniform heating achieved together with the lower capital cost compared to other electro heating methods such as microwave and radio frequency heating. The applications of Joule heating technique in industries include the blanching, evaporation, dehydration and pasteurization of food products. In view of these applications (Abo-Eldahab and El-Aziz [17], El-Aziz [18], Osalusi and Harris [19], Pal and Talukdar[20]) have studied the Joule heating effect involving problems.

Motivated by the above referenced works and the numerous possible industrial applications of engineering fields, it is of paramount interest in this study to analyze the MHD mixed convective slip flow of a heat absorbing fluid in a vertical plate. To the best of author's knowledge the influence of Soret effect on MHD mixed convective slip flow in a permeable vertical plate has not been studied before. Therefore the main objective of this study is to examine the influence of buoyancy, viscous dissipation, Joule heating and thermal diffusion effects on MHD mixed convective slip flow in a permeable vertical plate. Graphical display of the numerical examine is performed to illustrate the influence of various flow parameters on the velocity, temperature, concentration, skin friction coefficient, Nusselt number and Sherwood number distributions. The rest of the paper is structured as follows: we present the governing equations in Section 2. We proceed in Section 3 to solve the set of equations by using perturbation method. Section 4 provides a discussion of results and we present conclusions in Section 5.

Formulation of the problem

We consider the steady two-dimensional flow of an incompressible, viscous, electrically conducting and heat-observing fluid past a semi-infinite vertical permeable plate subject to slip boundary condition at the interface of fluid layers. In the momentum equation, a uniform transverse magnetic field of magnitude and buoyancy effect is considered. Energy equation includes the viscous dissipative and Joule heating

Tele:

E-mail addresses: rushikumar@vit.ac.in, Sivaraj.kpm@gmail.com

effects. The Soret effect is taken into account in the mass diffusion equation. Rest of properties of the fluid are assumed to be constant. Figure 1 depicts the flow geometry of this problem.

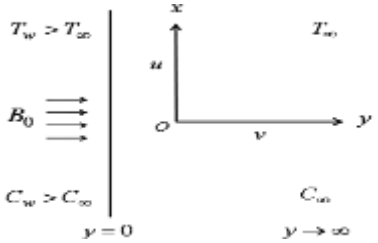

Figure 1: Flow geometry of the problem

The governing equations for this investigation are based on the balance laws of mass, linear momentum, energy and concentration species. Taking into consideration of these assumptions, the equations that describe the physical situation can be represented as follows:

$$\frac{\partial u}{\partial x}+\frac{\partial v}{\partial y}=0 \tag{1}$$

$$\left(u\frac{\partial u}{\partial x}+v\frac{\partial u}{\partial y}\right)=-\frac{1}{\rho}\frac{\partial p}{\partial x}+\nu\left(\frac{\partial^2 u}{\partial x^2}+\frac{\partial^2 u}{\partial y^2}\right) -\frac{\sigma B_0^2}{\rho}u+g\beta_T\left(T-T_\infty\right)+g\beta_C\left(C-C_\infty\right) \tag{2}$$

$$\left(u\frac{\partial T}{\partial x}+v\frac{\partial T}{\partial y}\right)=\frac{k}{\rho C_p}\left(\frac{\partial^2 T}{\partial x^2}+\frac{\partial^2 T}{\partial y^2}\right) -\frac{Q\left(T-T_\infty\right)}{\rho C_p}+\frac{\nu}{C_p}\left(\frac{\partial u}{\partial x}+\frac{\partial u}{\partial y}\right)^2+\frac{\sigma B_0^2 u^2}{\rho C_p} \tag{3}$$

$$\left(u\frac{\partial C}{\partial x}+v\frac{\partial C}{\partial y}\right)=D\left(\frac{\partial^2 C}{\partial x^2}+\frac{\partial^2 C}{\partial y^2}\right) +\frac{DK_T}{\bar{T}}\left(\frac{\partial^2 T}{\partial x^2}+\frac{\partial^2 T}{\partial y^2}\right) \tag{4}$$

The boundary conditions of this problem are

$$u=u_{slip}=\frac{\sqrt{K}}{\gamma_1}\frac{\partial u}{\partial y},\quad T=T_w,\quad C=C_w \quad at \quad y=0 \tag{5}$$

$$u\to u_\infty=0,\quad T_w\to T_\infty,\quad C_w\to C_\infty \quad as \quad y\to\infty \tag{6}$$

Since the motion is two dimensional and length of the plate is large enough. So, all the physical variables are independent of $x-$ axis. Therefore

$$\frac{\partial u}{\partial x}=0 \tag{7}$$

We consider that the suction velocity at the plate surface is constant and the suction velocity takes the following form:

$$v=-V_0 \tag{8}$$

Outside the boundary layer, Eqn. (2) gives

$$-\frac{1}{\rho}\frac{dp}{dx}=A \tag{9}$$

Introducing the following non-dimensional quantities

$$U=\frac{u}{U_0},\ V=\frac{v}{V_0},\ Y=\frac{V_0 y}{\nu},\ \theta=\frac{T-T_\infty}{T_w-T_\infty},\ \phi=\frac{C-C_\infty}{C_w-C_\infty},$$

$$Gr=\frac{\nu g\beta_T\left(T_w-T_\infty\right)}{U_0V_0^2},$$

$$Gc=\frac{\nu g\beta_C\left(C_w-C_\infty\right)}{U_0V_0^2},\ M^2=\frac{\sigma B_0^2\nu}{\rho V_0^2},$$

$$Pr=\frac{\mu C_p}{k},\ \alpha=\frac{Q\nu}{\rho C_p V_0^2},\ Sc=\frac{\nu}{D},$$

$$E=\frac{U_0^2}{C_p\left(T_w-T\infty\right)},\ Sr=\frac{K_T\left(T_w-T\infty\right)}{\bar{T}\left(C_w-C\infty\right)},$$

$$\gamma=\frac{\sqrt{K}U_0V_0}{\gamma_1\nu} \tag{10}$$

In view of the above non-dimensional variables, the basic equations (2) to (4) can be expressed in non-dimensional form as

$$\frac{d^2U}{dY^2}+\frac{dU}{dY}-M^2U+Gr\theta+Gc\phi+A=0 \tag{11}$$

$$\frac{d^2\theta}{dY^2}+Pr\frac{d\theta}{dY}-Pr\alpha\theta +PrE\left(\frac{dU}{dY}\right)^2+PrM^2EU^2=0 \tag{12}$$

$$\frac{d^2\phi}{dY^2}+Sc\frac{d\phi}{dY}+Sr\left(\frac{d^2\theta}{dY^2}\right)=0 \tag{13}$$

The boundary conditions become

$$U=U_{slip}=\gamma\frac{dU}{dY},\quad \theta=1,\quad \phi=1 \quad at \quad Y=0 \tag{14}$$

$$U\to 0,\ \theta\to 0,\ \phi\to 0 \ \ as \ \ Y\to\infty \tag{15}$$

The Eckert number is always less than unity since the flow due to the Joules dissipation is supper imposed on the main flow. So that we consider, $E=\in$.

Method of solution

The set of partial differential equations (11) to (15) cannot be solved in closed-form. However, it can be solved analytically after these equations are reduced to a set of ordinary differential equations in dimensionless form which can be done by representing the velocity U, temperature θ and concentration ϕ as

$$U(Y)=f_0(Y)+\in f_1(Y)+o\left(\in^2\right) \tag{17}$$

$$\theta(Y)=\theta_0(Y)+\in\theta_1(Y)+o\left(\in^2\right) \tag{18}$$

$$\phi(Y)=\phi_0(Y)+\in\phi_1(Y)+o\left(\in^2\right) \tag{19}$$

Substituting (17) to (19) into equations (11) to (15) and equating the corresponding terms of the equations, neglecting the higher order of $o\left(\in^2\right)$ and simplifying to get the following pairs of equations for $f_0,\ \theta_0,\ \phi_0$ and $f_1,\ \theta_1,\ \phi_1$.

$$f_0''+f_0'-M^2f_0=-\left(A+Gr\theta_0+Gc\phi_0\right) \tag{20}$$

$$f_1''+f_1'-M^2f_1=-\left(Gr\theta_1+Gc\phi_1\right) \tag{21}$$

$$\theta_0''+Pr\theta_0'-Pr\alpha\theta_0=0 \tag{22}$$

$$\theta_1'' + Pr\theta_1' - Pr\alpha\theta_1 = -\left(Pr\left(U_0'\right)^2 - PrMU_0^2\right) \quad (23)$$

$$\phi_0'' + Sc\phi_0' = -Sr\theta_0'' \quad (24)$$

$$\phi_1'' + Sc\phi_1' = -Sr\theta_1'' \quad (25)$$

The corresponding boundary conditions become

$$f_0 = \gamma_1 f_0',\ f_1 = \gamma_1 f_1',\ \theta_0 = 1,\ \theta_1 = 0,\ \phi_0 = 1,\ \phi_1 = 0 \quad at \quad Y = 0 \quad (26)$$

$$f_0 \to 0,\ f_1 \to 0,\ \theta_0 \to 0,\ \theta_1 \to 0,\ \phi_0 \to 0,\ \phi_1 \to 0 \quad as \quad Y \to \infty \quad (27)$$

The solutions of equations (20) to (25) subject to the boundary conditions (26) and (27) are

$$f_0 = A_3 e^{-\beta_1 Y} + A_4 e^{-\beta_2 Y} + A_6 e^{-\beta_3 Y} + A_5 \quad (28)$$

$$f_1 = A_{30}e^{-\beta_1 Y} + A_{31}e^{-\beta_2 Y} + A_{41}e^{-\beta_3 Y} + A_{33}e^{-2\beta_1 Y} + A_{34}e^{-2\beta_2 Y} + A_{35}e^{-2\beta_3 Y} + A_{36}e^{-(\beta_1+\beta_2)Y} + A_{37}e^{-(\beta_2+\beta_3)Y} + A_{38}e^{-(\beta_1+\beta_3)Y} \quad (29)$$

$$\theta_0 = e^{-\beta_1 Y} \quad (30)$$

$$\theta_1 = A_{17}e^{-\beta_1 Y} + A_8 e^{-\beta_2 Y} + A_9 e^{-\beta_3 Y} + A_{10}e^{-2\beta_1 Y} + A_{11}e^{-2\beta_2 Y} + A_{12}e^{-2\beta_3 Y} + A_{13}e^{-(\beta_1+\beta_2)Y} + A_{14}e^{-(\beta_2+\beta_3)Y} + A_{15}e^{-(\beta_1+\beta_3)Y} + A_{16} \quad (31)$$

$$\phi_0 = A_1 e^{-\beta_1 Y} + A_2 e^{-\beta_2 Y} \quad (32)$$

$$\phi_1 = A_{19}e^{-\beta_1 Y} + A_{29}e^{-\beta_2 Y} + A_{21}e^{-\beta_3 Y} + A_{22}e^{-2\beta_1 Y} + A_{23}e^{-2\beta_2 Y} + A_{24}e^{-2\beta_3 Y} + A_{25}e^{-(\beta_1+\beta_2)Y} + A_{26}e^{-(\beta_2+\beta_3)Y} + A_{27}e^{-(\beta_1+\beta_3)Y} \quad (33)$$

Substituting the above solutions (28) to (33) in (17) to (19) we get the final form of velocity, temperature and concentration distributions in the boundary layer as follows:

$$U(Y,t) = \begin{bmatrix} A_3 e^{-\beta_1 Y} + A_4 e^{-\beta_2 Y} \\ + A_6 e^{-\beta_3 Y} + A_5 \end{bmatrix} + \in \begin{bmatrix} A_{30}e^{-\beta_1 Y} + A_{31}e^{-\beta_2 Y} + A_{41}e^{-\beta_3 Y} \\ + A_{33}e^{-2\beta_1 Y} + A_{34}e^{-2\beta_2 Y} \\ + A_{35}e^{-2\beta_3 Y} + A_{36}e^{-(\beta_1+\beta_2)Y} \\ + A_{37}e^{-(\beta_2+\beta_3)Y} + A_{38}e^{-(\beta_1+\beta_3)Y} \end{bmatrix} \quad (34)$$

$$\theta(Y,t) = \left[e^{-\beta_1 Y}\right] + \in \begin{bmatrix} A_{17}e^{-\beta_1 Y} + A_8 e^{-\beta_2 Y} + A_9 e^{-\beta_3 Y} \\ + A_{10}e^{-2\beta_1 Y} + A_{11}e^{-2\beta_2 Y} + A_{12}e^{-2\beta_3 Y} \\ + A_{13}e^{-(\beta_1+\beta_2)Y} + A_{14}e^{-(\beta_2+\beta_3)Y} \\ + A_{15}e^{-(\beta_1+\beta_3)Y} + A_{16} \end{bmatrix} \quad (35)$$

$$\phi(Y,t) = \left[A_1 e^{-\beta_1 Y} + (1-A_1)e^{-\beta_2 Y}\right] + \in \begin{bmatrix} A_{19}e^{-\beta_1 Y} + A_{29}e^{-\beta_2 Y} + A_{21}e^{-\beta_3 Y} \\ + A_{22}e^{-2\beta_1 Y} + A_{23}e^{-2\beta_2 Y} \\ + A_{24}e^{-2\beta_3 Y} + A_{25}e^{-(\beta_1+\beta_2)Y} \\ + A_{26}e^{-(\beta_2+\beta_3)Y} + A_{27}e^{-(\beta_1+\beta_3)Y} \end{bmatrix} \quad (36)$$

The shear stress, the coefficient of the rate of heat transfer and the rate of mass transfer at any point in the fluid can be characterized by

$$\tau^* = \mu u';\ Nu^* = -kT';\ Sh^* = -DC' \quad (37)$$

In dimensionless form

$$\tau = \frac{\tau^*\rho}{U_0 V_0} = -u';\ Nu = \frac{Nu^*\nu}{k(T_w - T_\infty)V_0} = -\theta';$$

$$Sh = \frac{Sh^*\nu}{D(C_w - C_\infty)V_0} = -\phi' \quad (38)$$

The skin friction, the Nusselt number and the Sherwood number at the wall $y = 0$ is given by

$$\tau_0 = -u'|_{y=0};\ Nu_0 = -\theta'|_{y=0};\ Sh_0 = \phi'|_{y=0} \quad (39)$$

$$\tau_0 = -\left[A_2\beta_1 + A_3\beta_2 + A_4\beta_3\right] - \in e^{nt}\begin{bmatrix} A_{30}\beta_1 + A_{31}\beta_2 + A_{32}\beta_3 \\ +2A_{33}\beta_1 + 2A_{34}\beta_2 + \\ 2A_{35}\beta_3 + A_{36}(\beta_1+\beta_2) + \\ A_{37}(\beta_2+\beta_3) + A_{38}(\beta_1+\beta_3) \end{bmatrix} \quad (40)$$

$$Nu_0 = -\beta_1 - \in \begin{bmatrix} A_{17}\beta_1 + A_8\beta_2 + A_9\beta_3 \\ +2A_{10}\beta_1 + 2A_{11}\beta_2 \\ +2A_{12}\beta_3 + A_{13}(\beta_1+\beta_2) + \\ A_{14}(\beta_2+\beta_3) + A_{15}(\beta_1+\beta_3) \end{bmatrix} \quad (41)$$

$$Sh_0 = -\left[A_1\beta_1 + A_2\beta_2\right] - \in \begin{bmatrix} A_{19}\beta_1 + A_{29}\beta_2 + A_{21}\beta_3 \\ +2A_{22}\beta_1 + 2A_{23}\beta_2 \\ +2A_{24}\beta_3 + A_{25}(\beta_1+\beta_2) + \\ A_{26}(\beta_2+\beta_3) + A_{27}(\beta_1+\beta_3) \end{bmatrix} \quad (42)$$

where the prime denotes ordinary differentiation with respect to Y, A's and β's are given in Appendix.

Result and Discussion

Graphical representation of results is very useful to discuss the physical features presented by the solutions. In order to get a physical insight into the problem, factors such as velocity, temperature, concentration, Skin friction, Nusselt number and Sherwood number have been discussed by assigning numerical values to various parameters obtained in the mathematical formulation of the problem and the results are graphically shown in figures 2 - 21. Throughout the computations we employ $\in = 0.2$, $A = 0.02$, $M = 2$, $\gamma = 0.3$, $Gr = 4$, $Gr = 2$, $Gc = 2$, $\alpha = 2$, $\Pr = 0.71$, $Sc = 1$ and $Sr = 0.5$ unless otherwise stated. The velocity distribution against Y for different values of the parameters M, γ, Gr, Gc, α, $\Pr$, Sr and Sc are graphically displayed in figures 2-9. The

application of magnetic field moving with the free stream has the tendency to induce a motive force which decreases the motion of the fluid which is presented in figure 2. It is clear from the figure 3 that increase in porous permeability parameter has the tendency to reduce the friction forces and increase the velocity profile. Usually the thermal Grashof number and solutal Grashof number boost the fluid velocity. It is found that the effect of increasing thermal Grashof number and solutal Grashof number increase the velocity field as expected which is displayed in figures 4&5. It is seen that increasing heat absorption parameter and Prandtl number diminish the velocity significantly which is shown in figures 6&7. Figure 8 displays that increase in the Soret number significantly increase the fluid velocity throughout the boundary layer. The values of the Schmidt number are chosen to represent the presence of species by hydrogen (0.24), water vapor (0.6), ammonia (0.78), carbon dioxide (1) and ethyl benzene (2). Figure 9 display the velocity profiles for different values of Sc. It is seen from this figure that the velocity profiles decrease monotonically with the increase of Schmidt number. Temperature distribution against Y for different values of the parameters α, Pr, Sc and Sr are graphically presented in figures 10-13. Figure 10 represents that increase in the heat absorption parameter has tendency to decrease heat transfer because it acts against the thermal buoyancy effects. Figure 11 presents that increase in Prandtl number equivalent to increase the thermal conductivities and therefore heat is able to diffuse away from the heated plate more rapidly. Hence in the case of increasing Prandtl numbers, the boundary layer is thicker and the rate of heat transfer is reduced. The heat transfer falls off for the rise of Schmidt number which is depicted in figure12. Increase in Soret number enhances heat transfer which is plotted in figure 13. Concentration distribution against Y for different values of the parameters Sc and Sr are shown in the figures 14&15. Figure 14 shows that the increase in Schmidt number decrease the concentration profiles. Physically, the increase of Schmidt number means decrease of molecular diffusion. Hence, the mass transfer of the species is higher for small values of Schmidt number and lower for larger values of Schmidt number. It is observed from Figure 15 that the concentration increases for increasing Soret number. Hence, it is an evident that the Soret number can't be negligible in the heat and mass transfer of lower molecular weight fluids. We present the variation of the effect of skin friction co-efficient against the thermal Grashof number for various values of γ and Gc through the figures 16&17. It is noticed from figure 16 that value of the shearing stress falls rapidly for the rise of porous permeability parameter. The increments of mass Grashof number increase the skin friction which is shown in figure 17. The Nusselt number against the magnetic field parameter for various values of α and Pr are graphically displayed in figures 18&19. It is observed that increase in heat absorption parameter and Prandtl number cause to decrease the rate of heat transfer. The Sherwood number subject to M for various values of Sc and Sr are presented graphically in figures 20&21. The rate of mass transfer decreases for increasing the Schmidt number but the Soret number reverse the effect.

Tables 1 to 4 are presented to show the influence of Gr, Gc, α and Sc in skin friction, Nusselt number and Sherwood number distributions. Tables 1 & 2 show that increase in the thermal and mass Grashof number increases the skin friction and Nusselt number where as it decreases the Sherwood number. In Table 3, with increase in the heat absorption parameter there is a slight decrease in the values of the skin friction and Nusselt number. The Sherwood number increases with increase in the heat absorption parameter. Table 4 shows that increase in the Soret number increases the values of the skin friction, Nusselt number and Sherwood number.

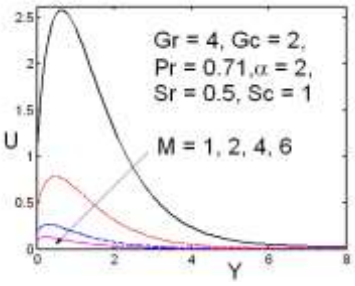

Figure 2: Effect of magneic field in velocity distribution

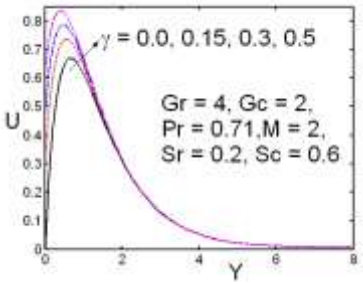

Figure 3: Effect of porous permiability in velocity distribution

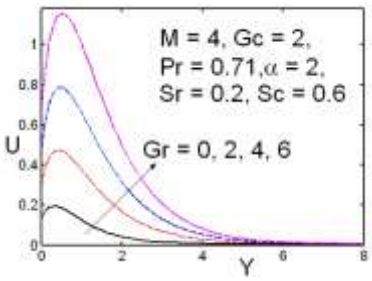

Figure 4: Effect of thermal Grashof number in velocity distribution

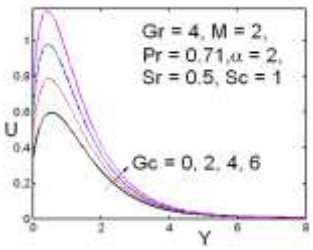

Figure 5: Effect of solutal Grashof number in velocity distribution

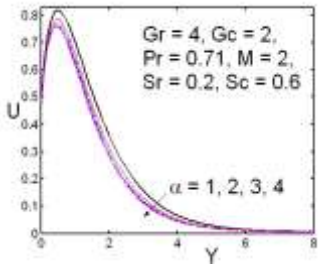

Figure 6: Effect of heat absorbtion parameter in velocity distribution

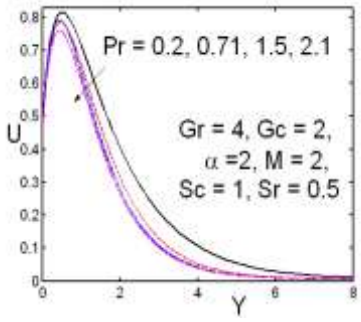

Figure 7: Effect of Prandtl number in velocity distribution

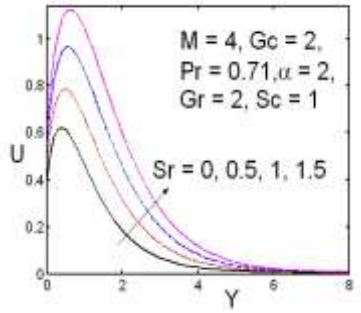

Figure 8: Effect of Soret number in velocity distribution

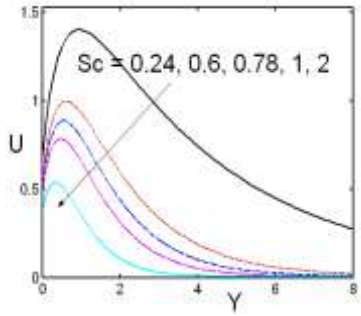

Figure 9: Effect of Schmidt number in velocity distribution

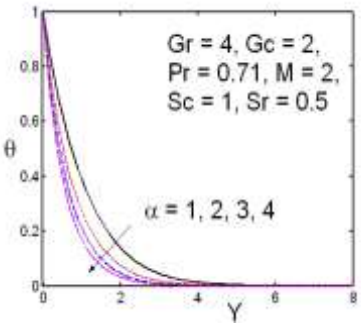

Figure 10: Effect of heat absorbtion parameter in temperature distribution

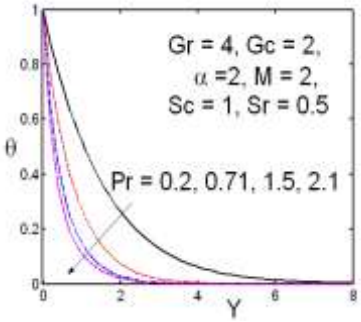

Figure 11: Effect of Prandtl number in temperature distribution

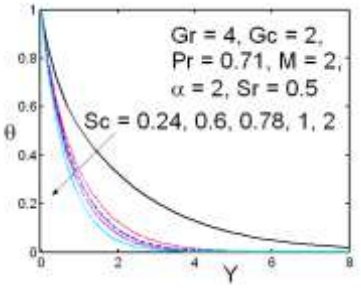

Figure 12: Effect of Schmidt number in temperature distribution

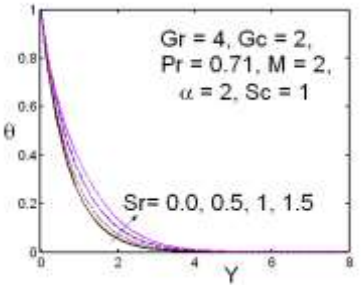

Figure 13: Effect of Soret number in temperature distribution

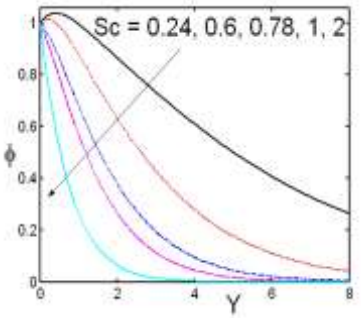

Figure 14: Effect of Schmidt number in concentration distribution

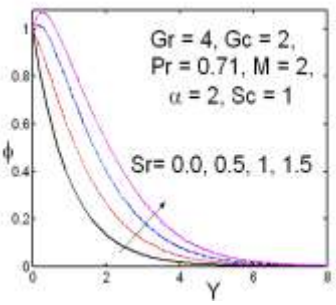

Figure 15: Effect of Soret number in concentration distribution

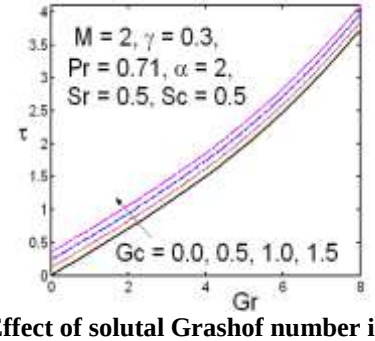

Figure 16: Effect of solutal Grashof number in skin friction distribution

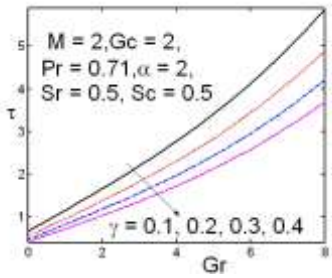

Figure 17: Effect of porous permiability parameter in skin friction distribution

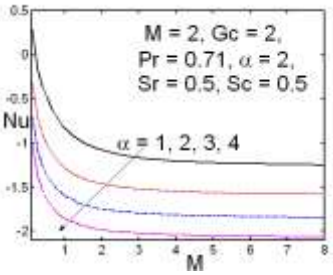

Figure 18: Effect of heat absorption parameter in Nusselt number distribution

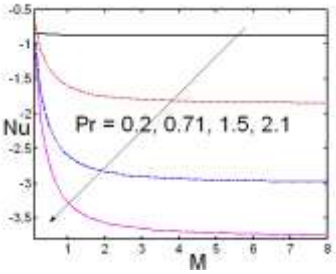

Figure 19: Effect of Prandtl number in Nusselt number distribution

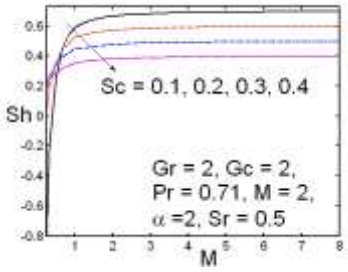

Figure 20: Effect of Schmidt number in Sherwood number distribution

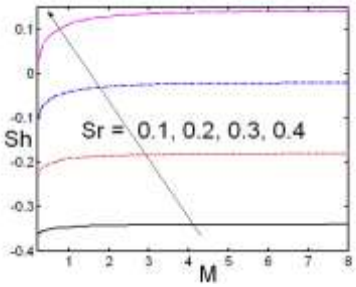

Figure 21: Effect of Soret number in Sherwood number distribution

Conclusions

We have analyzed the steady MHD mixed convective slip flow in a permeable vertical plate with buoyancy, Joule heating and Soret effect. A comprehensive set of graphical results for the velocity, temperature and concentration profiles are presented and discussed. Velocity profiles increase with the increase of Grashof number, modified Grashof number, Soret number and permeability parameter. Velocity decreases with an increase in magnetic parameter, Schmidt number, Prandtl number and heat absorption parameter.

Increase in heat absorption parameter and Prandtl number diminish the fluid temperature.

The heat and mass transfer increases for increasing Soret number. Also, with increase in the thermal diffusion (Soret number) the rate of mass transfer increases but the increases in the Schmidt number decrease the rate of mass transfer.

It is more realistic to include Joule heating in order to explore the impact of the magnetic field on the thermal transport in the boundary layer. It is observed that the agreement with the theoretical solutions of all profiles is excellent.

References

[1] Barletta A, Lazzari S, Magyari E, Pop I. Mixed convection with heating effects in a vertical porous annulus with a radially varying magnetic field. Int J of Heat and Mass Transfer. 2008; 51: 5777–84.

[2] Afify A. Similarity solution in MHD effects of thermal diffusion and diffusion thermo on free convective heat and mass transfer over a stretching surface considering suction or injection. Commun Nonlinear Sci Numer Simulat. 2009; 14(5): 2202–14.

[3] Srinivas S, Muthuraj R, Effects of thermal radiation and space porosity on MHD mixed convection flow in a vertical channel using homotopy analysis method. Commun Nonlinear Sci Numer Simulat 2010; 15: 2098–108

[4] Prakash J, Sivaraj R, Rushi Kumar B. Influence of chemical reaction on unsteady MHD mixed convective flow over a moving vertical porous plate. Int J of Fluid Mechanics. In press, Article No. 2, 2011.

[5] Yih KA. The effect of transpiration on coupled heat and mass transfer in mixed convection over a vertical plate embedded in a saturated porous medium. Int Commun in Heat and Mass Transfer. 1997; 24(2): 265–75.

[6] Barletle A. Combined forced and free convection with viscous dissipation in a vertical duct. Int J Heat and Mass Transfer. 1999; 42: 2243–53.

[7] Chin KE, Nazar R, Arifin NM, Pop I. Effect of variable viscosity on mixed convection boundary layer flow over a vertical surface embedded in a porous medium. Int Commun in Heat and Mass Transfer. 2007; 34(4): 464–73.

[8] Motsa SS. The Effects of Thermal Radiation, Hall currents, Soret, and Dufour on MHD flow by mixed convection over a vertical surface in porous media. SAMSA Journal of Pure and Applied Mathematics. 2008; 3: 58–65.

[9] Kafoussias NG, Williams EW. Thermal-diffusion and diffusion-thermo effects on mixed free forced convective and mass transfer boundary layer flow with temperature dependent viscosity. Int J of Engineering Science 1995; 33(9): 1369–84.

[10] Angel M, Takhar HS, Pop I. Dofour and Soret effects on free convection boundary layer over a vertical surface embedded in a porous medium. Studia universities- Bolyai. Mathematica 2000. 45: 11–21.

[11] Alam MS, Rahman MM. Dufour and Soret effects on mixed convection flow past a vertical porous flat plate with variable suction. Nonlinear Analysis: Modelling and Control. 2006; 11(1): 3–12.

[12] Mansour MA, El-Anssary NF, Aly AM. Effects of chemical reaction and thermal stratification on MHD free convective heat and mass transfer over a vertical stretching surface embedded in

a porous media considering Soret and Dufour numbers. Chemical Engineering J. 2008; 145: 340–345.
[13] Alimi SE, Orfi J, Nasrallah Sb. Buoyancy effects on mixed convection heat and mass transfer in a duct with sudden expansions, Heat Mass Transfer. 2005; 41: 559–67.
[14] Shateyi S. Thermal radiation and buoyancy effects on heat and mass transfer over a semi-infinite stretching surface with suction and blowing. J of Applied Mathematics. 2008; Article ID 414830.
[15] Elzubier AS, Thomas SYC, Sergie SY, Chin NL, Ibrahim OM. The effect of buoyancy force in computational fluid dynamics simulation of a two-dimensional continuous ohmic heating process. American J of Applied Sciences. 2009; 6(11): 1902–8.
[16] Muthuraj R, Srinivas S. Mixed convective heat and mass transfer in a vertical wavy channel with traveling thermal waves and porous medium. Computers and Mathematics with Applications. 2010; 59: 3516–28.
[17] Abo-Eldahab EM, El-Aziz AM. Hall current and Ohmic heating effects on mixed convection boundary layer flow of a mixpolar fluid from a rotating cone with power-law variation in surface temperature. Int Commun Heat Mass Transfer. 2004; 31: 751–62.
[18] El-Aziz AM. Temperature dependent viscosity and thermal conductivity effects on combined heat and mass transfer in MHD three dimensional flow over a stretching surface with Ohmic heating. Meccanica. 2007; 42: 375–86.
[19] Osalusi JS, Harris R. Thermal-diffusion and diffusion-thermo effects on combined heat and mass transfer of a steady MHD convective and slip flow due to a rotating disk with viscous dissipation and Ohmic heating. Int Commun in Heat and Mass Transfer. 2008; 35(8): 908–15.
[20] Pal D, Talukdar B. Buoyancy and chemical reaction effects on MHD mixed convection heat and mass transfer in a porous medium with thermal radiation and Ohmic heating. Commun Nonlinear Sci Numer Simulat. 2010; 15(10): 2878–93.

Appendix

$$\beta_1=\frac{Pr+\sqrt{Pr^2+4Pr\alpha}}{2},\ \beta_2=Sc,$$

$$\beta_3=\frac{1+\sqrt{1+4M}}{2},\ A_1=\frac{Sr\beta_1}{\beta_2-\beta_1},$$

$$A_2=(1-A_1),\ \ A_3=\frac{-(A_1Gr+Gc)}{\beta_1^2-\beta_1-M^2},\ A_4=\frac{-A_2Gr}{\beta_2^2-\beta_2-M^2},$$

$$A_5=\frac{A}{M^2},\ \ A_6=\frac{-\left[A_3+A_4+A_5+\gamma(A_3\beta_1+A_4\beta_2)\right]}{1+\gamma\beta_3},$$

$$A_7=\frac{-2A_3A_5PrM^2}{\beta_1^2-Pr\beta_1-Pr\alpha},$$

$$A_8=\frac{-2A_4A_5PrM^2}{\beta_2^2-Pr\beta_2-Pr\alpha},\ A_9=\frac{-2A_5A_6PrM^2}{\beta_3^2-Pr\beta_3-Pr\alpha},$$

$$A_{10}=\frac{-A_3^2Pr\left(\beta_1^2+M^2\right)}{4\beta_1^2-2Pr\beta_1-Pr\alpha},$$

$$A_{11}=\frac{-A_4^2Pr\left(\beta_2^2+M^2\right)}{4\beta_2^2-2Pr\beta_2-Pr\alpha},$$

$$A_{12}=\frac{-A_6^2Pr\left(\beta_3^2+M^2\right)}{4\beta_3^2-2Pr\beta_3-Pr\alpha},$$

$$A_{13}=\frac{-2A_3A_4Pr\left(\beta_1\beta_2+M^2\right)}{(\beta_1+\beta_2)^2-Pr(\beta_1+\beta_2)-Pr\alpha},$$

$$A_{14}=\frac{-2A_4A_6Pr\left(\beta_2\beta_3+M^2\right)}{(\beta_2+\beta_3)^2-Pr(\beta_2+\beta_3)-Pr\alpha},$$

$$A_{15}=\frac{-2A_3A_6Pr\left(\beta_1\beta_3+M^2\right)}{(\beta_1+\beta_3)^2-Pr(\beta_1+\beta_3)-Pr\alpha},$$

$$A_{16}=\frac{A_5^2M^2}{\alpha},\ A_{17}=-\left(A_7+A_8+A_9+....+A_{16}\right),$$

$$A_{18}=\left(A_7+A_{17}\right),\ A_{19}=\frac{-A_{18}Sr\beta_1^2}{\beta_1^2-Sc\beta_1},$$

$$A_{20}=\frac{-A_8Sr\beta_2^2}{\beta_2^2-Sc\beta_2},\ A_{21}=\frac{-A_9Sr\beta_3^2}{\beta_3^2-Sc\beta_3},$$

$$A_{22}=\frac{-4A_{10}Sr\beta_1^2}{4\beta_1^2-2Sc\beta_1},\ A_{23}=\frac{-4A_{11}Sr\beta_2^2}{4\beta_2^2-2Sc\beta_2},$$

$$A_{24}=\frac{-4A_{12}Sr\beta_3^2}{4\beta_3^2-2Sc\beta_3},$$

$$A_{25}=\frac{-A_{13}Sr(\beta_1+\beta_2)^2}{(\beta_1+\beta_2)^2-Sc(\beta_1+\beta_2)},$$

$$A_{26}=\frac{-A_{14}Sr(\beta_2+\beta_3)^2}{(\beta_2+\beta_3)^2-Sc(\beta_2+\beta_3)},$$

$$A_{27}=\frac{-A_{15}Sr(\beta_1+\beta_3)^2}{(\beta_1+\beta_3)^2-Sc(\beta_1+\beta_3)},$$

$$A_{28}=-\left(A_{19}+A_{20}+A_{21}....+A_{27}\right),$$

$$A_{29}=\left(A_{20}+A_{28}\right),\ A_{30}=\frac{-\left(A_{18}Gr+A_{19}Gc\right)}{\beta_1^2-\beta_1-M^2},$$

$$A_{31}=\frac{-\left(A_8Gr+A_{29}Gc\right)}{\beta_2^2-\beta_2-M^2},\ A_{32}=\frac{-\left(A_9Gr+A_{21}Gc\right)}{\beta_3^2-\beta_3-M^2},$$

$$A_{33}=\frac{-\left(A_{10}Gr+A_{22}Gc\right)}{4\beta_1^2-2\beta_1-M^2},\ A_{34}=\frac{-\left(A_{11}Gr+A_{23}Gc\right)}{4\beta_2^2-2\beta_2-M^2},$$

$$A_{35}=\frac{-\left(A_{12}Gr+A_{24}Gc\right)}{4\beta_3^2-2\beta_3-M^2},$$

$$A_{36}=\frac{-\left(A_{13}Gr+A_{25}Gc\right)^2}{(\beta_1+\beta_2)^2-(\beta_1+\beta_2)-M^2},$$

$$A_{37}=\frac{-\left(A_{14}Gr+A_{26}Gc\right)^2}{(\beta_2+\beta_3)^2-(\beta_2+\beta_3)-M^2},$$

$$A_{38}=\frac{-\left(A_{15}Gr+A_{27}Gc\right)^2}{(\beta_1+\beta_3)^2-(\beta_1+\beta_3)-M^2},$$

$$A_{39}=\frac{A_{16}Gr}{M^2},$$

$$A_{40}=\frac{-1}{1+\gamma\beta_3}\left[\begin{array}{l}\left(A_{30}+A_{31}+A_{32}+....+A_{39}\right)+\\ \gamma\left(\begin{array}{l}A_{30}\beta_1+A_{31}\beta_2+A_{32}\beta_3+\\ 2A_{33}\beta_1+2A_{34}\beta_2+2A_{35}\beta_3\\ +A_{36}(\beta_1+\beta_2)+\\ A_{37}(\beta_2+\beta_3)+A_{38}(\beta_1+\beta_3)\end{array}\right)\end{array}\right]\ A_{41}=\left(A_{32}+A_{40}\right)$$

Table 1: Effect of Gr in τ_0, Nu_0 & Sh_0

Gr	τ_0	Nu_0	Sh_0
0.0000	0.4746	-1.5901	0.1950
1.0000	0.8199	-1.5453	0.1722
2.0000	1.1772	-1.4613	0.1299
3.0000	1.5578	-1.3381	0.0679

Table 2: Effect Of Gc In τ_0, Nu_0 & Sh_0

Gc	τ_0	Nu_0	Sh_0
0.0000	0.7108	-1.5170	0.1577
0.5000	0.8277	-1.5048	0.1516
1.0000	0.9445	-1.4914	0.1450
1.5000	1.0610	-1.4769	0.1377

Table 3: Effect Of α In τ_0, Nu_0 & Sh_0

α	τ_0	Nu_0	Sh_0
1.0000	1.2105	-1.0796	-0.0617
2.0000	1.1772	-1.4613	0.1299
3.0000	1.1568	-1.7460	0.2725
4.0000	1.1422	-1.9825	0.3908

Table 4: Effect Of Sr In τ_0, Nu_0 & Sh_0

Sr	τ_0	Nu_0	Sh_0
0.0000	1.0370	-1.5140	-0.6000
0.5000	1.1772	-1.4613	0.1299
1.0000	1.3101	-1.3942	0.7921
1.5000	1.4321	-1.3130	1.3652